Cap completion and CTD kinase recruitment underlie the initiation-elongation transition of RNA polymerase II

Michael Lidschreiber,[1] Kristin Leike,[1] and Patrick Cramer[1]

[1]*Gene Center Munich and Department of Biochemistry, Center for Integrated Protein Science CIPSM, Ludwig-Maximilians-Universität München, Feodor-Lynen-Strasse 25, 81377 Munich, Germany.*

Supplemental Material

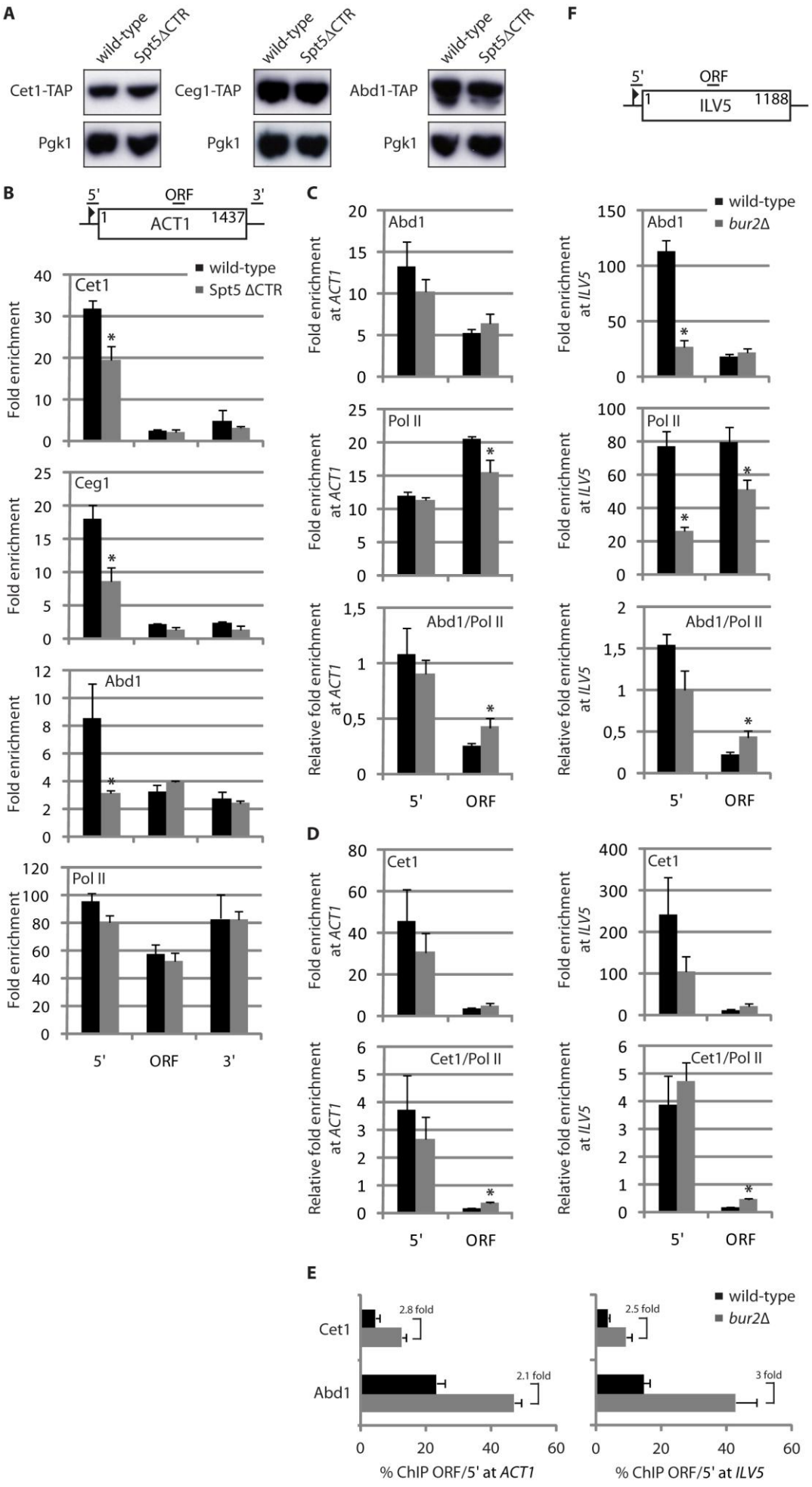
A
wild-type
Spt5ΔCTR
Cet1-TAP
Pgk1
Ceg1-TAP
Abd1-TAP
B
5'
ORF
3'
1
ACT1
1437
wild-type
Spt5 ΔCTR
Cet1
Ceg1
Abd1
Pol II
Fold enrichment
5'
ORF
3'
C
Abd1
Pol II
Abd1/Pol II
Fold enrichment at ACT1
Relative fold enrichment at ACT1
5'
ORF
D
Cet1
Cet1/Pol II
E
2.8 fold
2.1 fold
2.5 fold
3 fold
bur2Δ
% ChIP ORF/5' at ACT1
% ChIP ORF/5' at ILV5
F
ILV5
1188
Fold enrichment at ILV5
Relative fold enrichment at ILV5

Figure S1 The Spt5 CTR is involved in capping enzyme recruitment. (**A**) Western blot analyses showing equal levels of Cet1-TAP, Ceg1-TAP and Abd1-TAP in wild-type and Spt5ΔCTR cells under normal growth conditions. 40 µg of total protein were loaded from each strain. Pgk1 is included as an internal loading control. (**B**) ChIP-qPCR analysis was performed to monitor capping enzyme and Pol II recruitment at three different gene regions of *ACT1*: TSS (5′), coding (ORF, open reading frame) and terminator region (3′). Cet1, Ceg1, Abd1 and Pol II occupancies for wild-type (black bars) compared to Spt5ΔCTR (gray bars) cells are shown. Occupancies were calculated as fold enrichments over an ORF-free untranscribed region on chromosome V and are indicated on the y-axes (see Methods). Error bars show SD from three independent experiments of biological replicates, and the asterix (*) indicates if the factor occupancies are significantly different (p-value < 0.05) between the wild-type and mutant condition using Student's t-test. (**C**) ChIP-qPCR analysis as in **B** investigating two different gene regions of *ACT1* (left) and *ILV5* (**F**, right). Abd1 and Pol II occupancies for wild-type (black bars) compared to *bur2*Δ (gray bars) cells are shown. Abd1 fold enrichments relative to Pol II (Abd1/Pol II) were calculated by dividing Abd1 occupancies by Pol II occupancies. (**D**) Occupancies as in **C** for Cet1. (**E**) Cet1/Pol II and Abd1/Pol II ChIP signals for the ORF region of *ACT1* (left) and *ILV5* (right) relative to the ChIP signals at the 5' end of the genes.

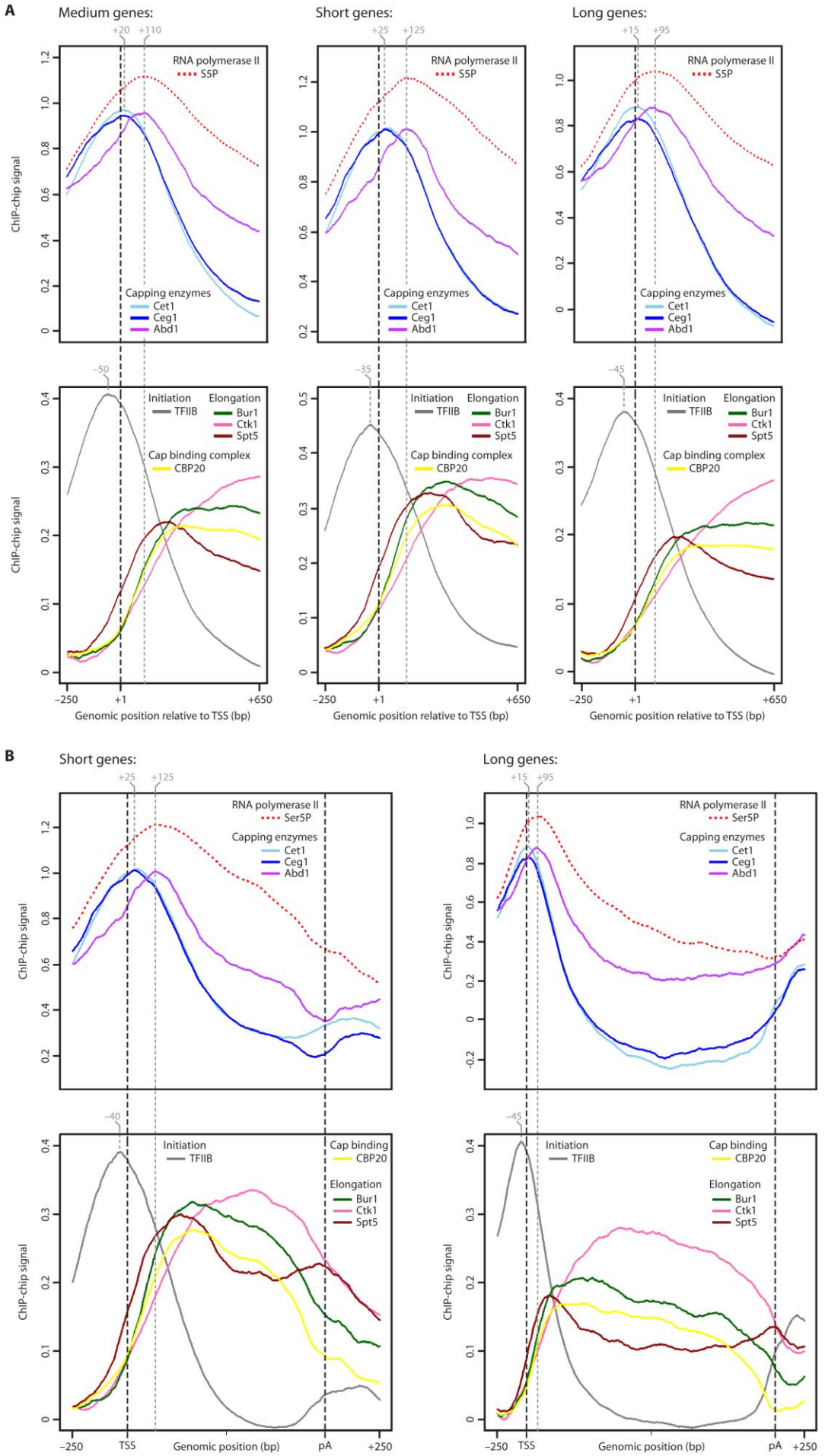
A
Medium genes:
Short genes:
Long genes:
RNA polymerase II
S5P
Capping enzymes
Cet1
Ceg1
Abd1
Initiation
TFIIB
Elongation
Bur1
Ctk1
Spt5
Cap binding complex
CBP20
ChIP-chip signal
Genomic position relative to TSS (bp)
B
Short genes:
Long genes:
RNA polymerase II
Ser5P
Capping enzymes
Cet1
Ceg1
Abd1
Initiation
TFIIB
Cap binding
CBP20
Elongation
Bur1
Ctk1
Spt5
ChIP-chip signal
TSS
pA
Genomic position (bp)

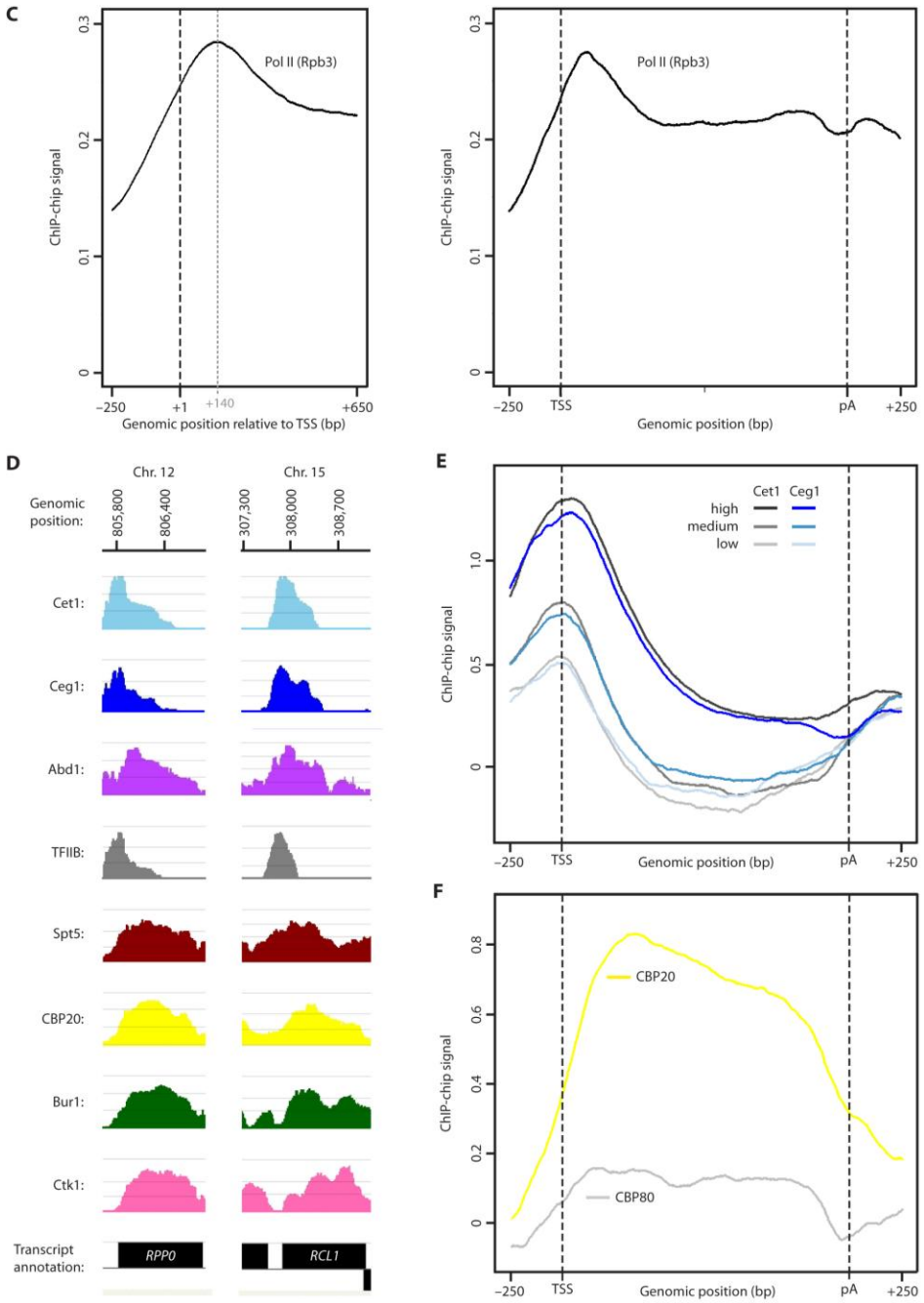

Figure S2 Genome-wide occupancy profiling of the capping machinery. (**A**) Gene-averaged ChIP-chip profiles for capping enzymes and Pol II phosphorylated at serine 5 (S5P) residues of the CTD (upper panel), and for initiation factor TFIIB, CBC subunit CBP20, and elongation factors Bur1, Ctk1 and Spt5 (lower panel). Occupancy profiles taken from the quality-filtered short (725 ± 213 bp, n = 266), medium (1238 ± 300 bp, n = 339), and long (2,217 ± 679 bp, n = 299) gene sets were cut around the TSS (250 bp upstream to 650 bp downstream; only genes > 680 bp were considered) and averaged using a 5% trimmed mean at each genomic position. ChIP-chip signal intensity is expressed as log2 IP/Input. For details refer to Methods. Dashed gray lines mark the peak positions of the averaged ChIP-chip profiles. (**B**) Gene-averaged ChIP-chip profiles as in **A**. Short and long genes were aligned at their TSS and pA sites, scaled to median length, and averaged using a 5% trimmed mean at each genomic position. For details refer to Methods. (**C**) Gene-averaged ChIP-chip profiles as in **A** and **B** for the Rpb3 subunit of Pol II. The left and right panels show the ALL gene set and medium length genes, respectively. (**D**) Gene tracks showing input normalized ChIP-chip occupancies for the capping machinery and transcription initiation and elongation factors at two example genes. (**E**) Gene-averaged profiles as in **B** for Cet1 and Ceg1 for genes in three different expression level classes. The quality-filtered set of medium length genes (Fig. 2) was partitioned into three groups: low (25%-50% quantile), medium (50%-75% quantile), and high (>75% quantile) expression level (Fig. 3 and Methods). (**F**) Gene-averaged ChIP-chip profiles for the cap binding complex subunits CBP20 (yellow) and CBP80 (gray). Since ChIP-chip signals for CBP80 were weak, only highly expressed genes as defined in (**E**) are shown.

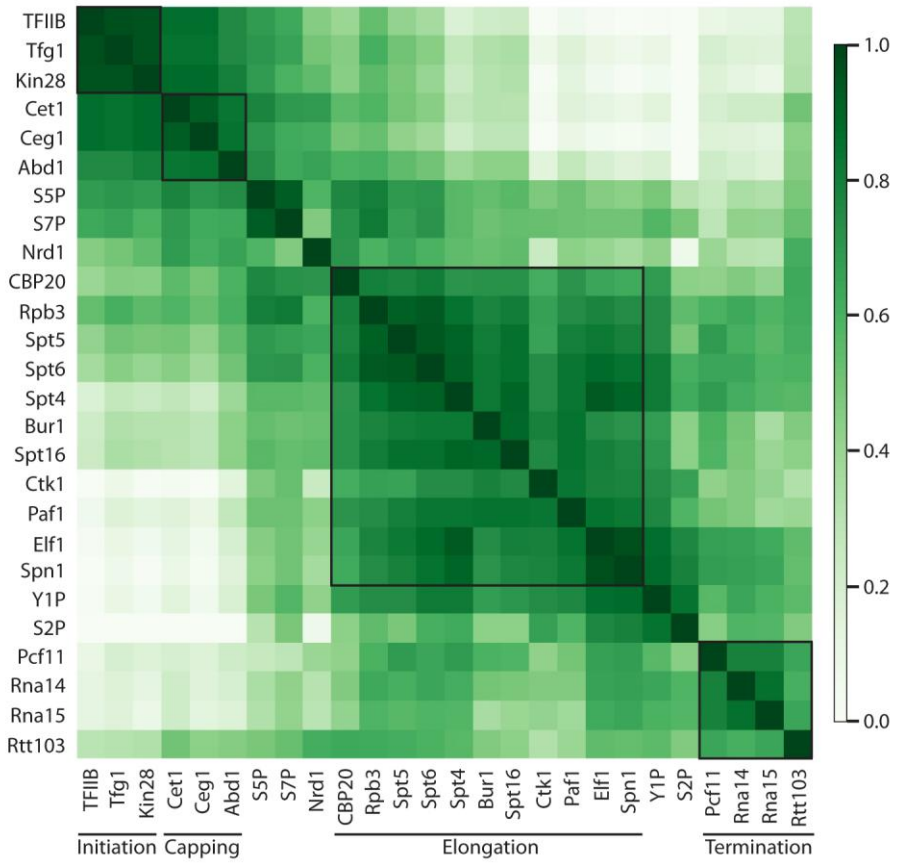

Figure S3 Correlation analysis of genome-wide occupancy profiles. Heatmap showing pairwise Pearson correlations between genome-wide ChIP-chip profiles (see Table S1). Correlation coefficients were calculated between concatenated gene profiles ranging each from TSS-250 bp to pA+250 bp (see Methods).

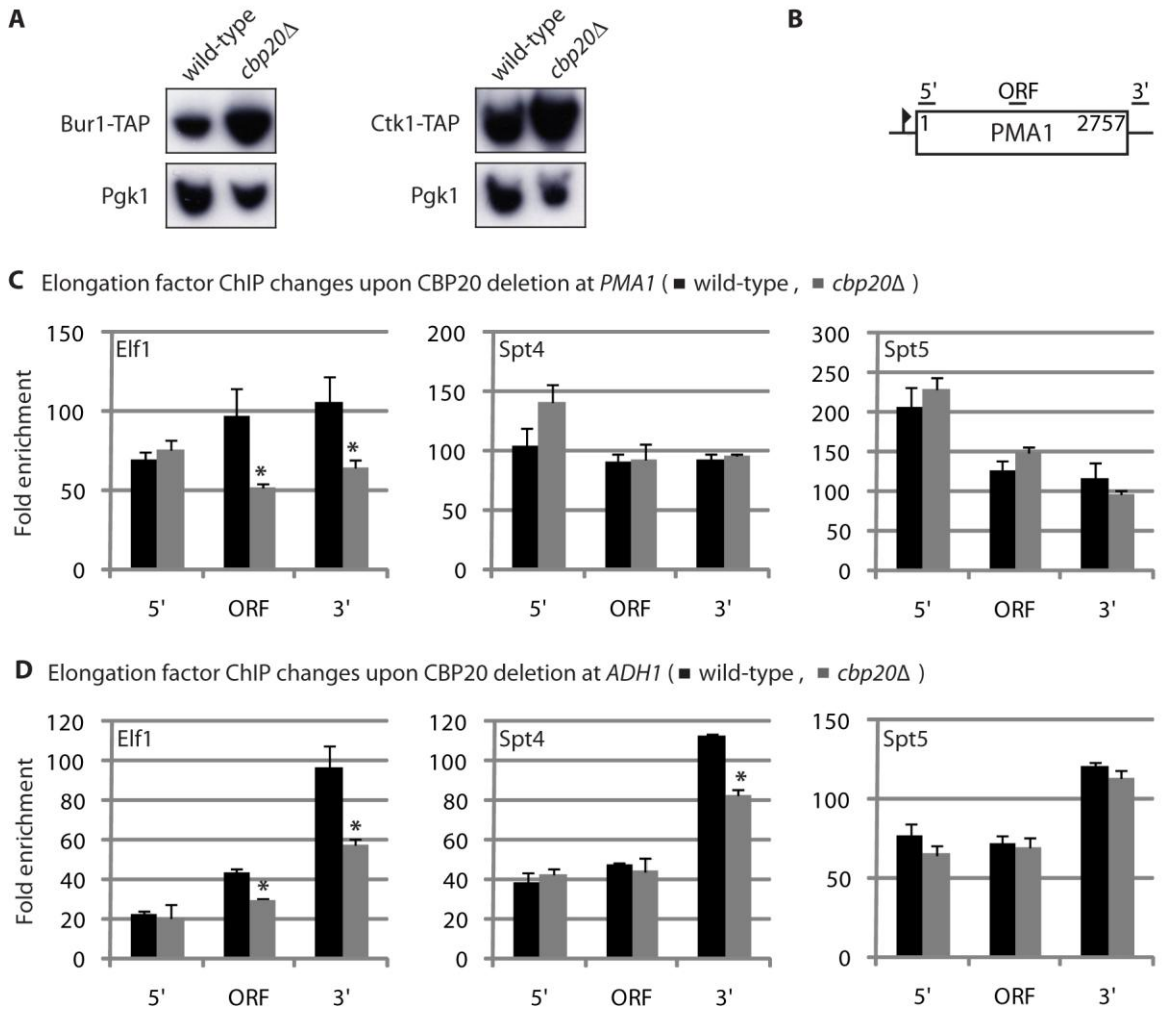

Figure S4 CBP20 is required for recruitment of kinases Bur1 and Ctk1. (**A**) Western blot analyses showing increased levels of Bur1-TAP and Ctk1-TAP in *cbp20*Δ compared to wild-type cells under normal growth conditions. 40 µg of total protein were loaded from each strain. Pgk1 is included as an internal loading control. (**B – D**) ChIP-qPCR analysis was performed to monitor changes in elongation factor recruitment upon CBP20 deletion. Three gene regions of *PMA1* (**B**, **C**) and *ADH1* (**D**, Fig.1) were investigated. Occupancies for wild-type (black bars) compared to *cbp20*Δ (gray bars) cells are shown. Occupancies were calculated as fold enrichments over an ORF-free untranscribed region on chromosome V and are indicated on the y-axes (see Methods). Error bars show SD from at least three independent experiments of biological replicates, and the asterix (*) indicates if the factor occupancies are significantly different (p-value < 0.05) between the wild-type and mutant condition using Student's t-test.

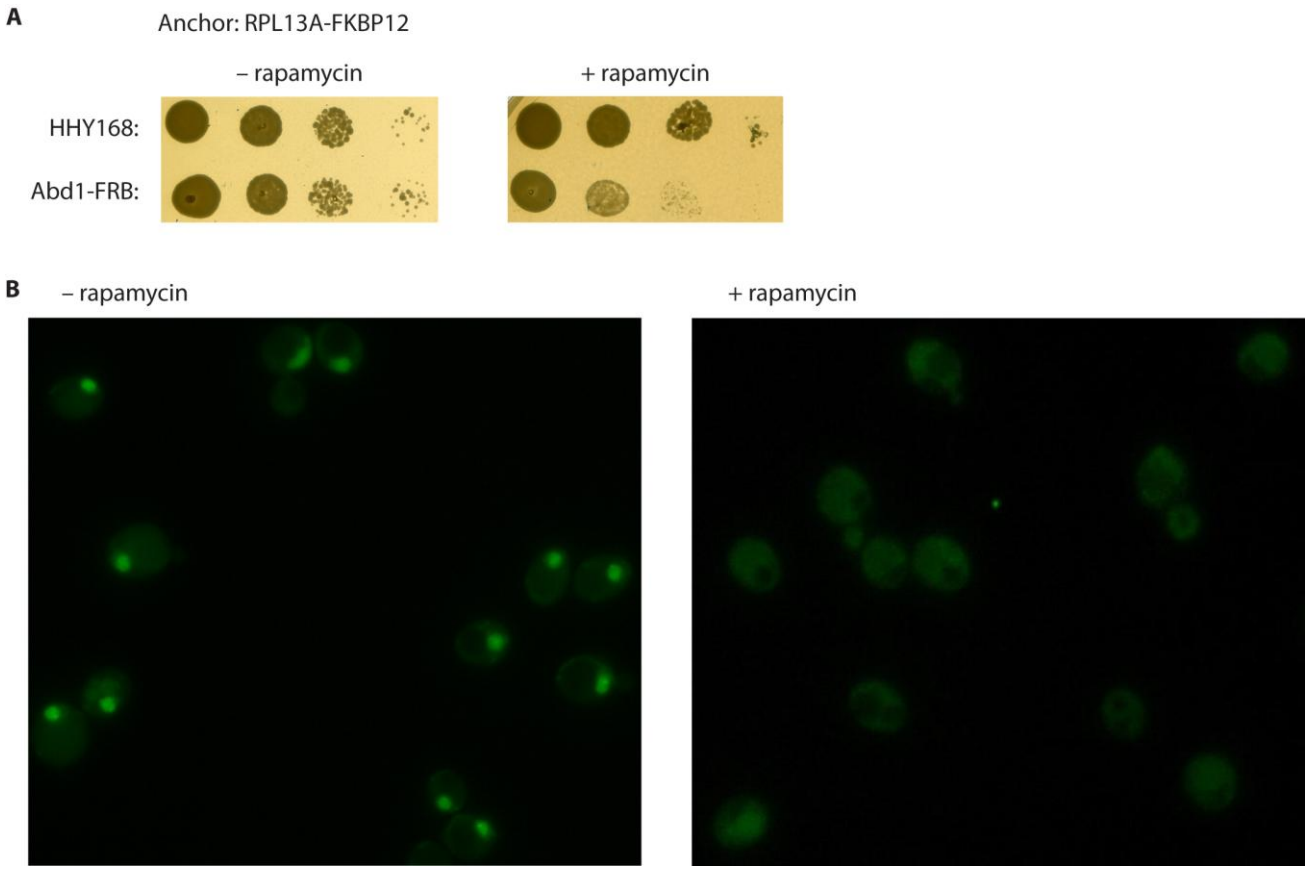

Figure S5 Rapamycin treatment leads to nuclear depletion of Abd1 and causes growth delay. (**A**) Spot dilution assay on YPD plates in the absence or presence of 1µg/ml f.c. rapamycin, respectively. The parental strain HHY168 was used as negative control. Dilutions were 10-fold. (**B**) GFP fluorescence of Abd1-FRB-GFP cells incubated without or with rapamycin (1µg/ml f.c. in DMSO) for 60 min, respectively. Addition of rapamycin causes depletion of Abd1-FRB-GFP from the nucleus.

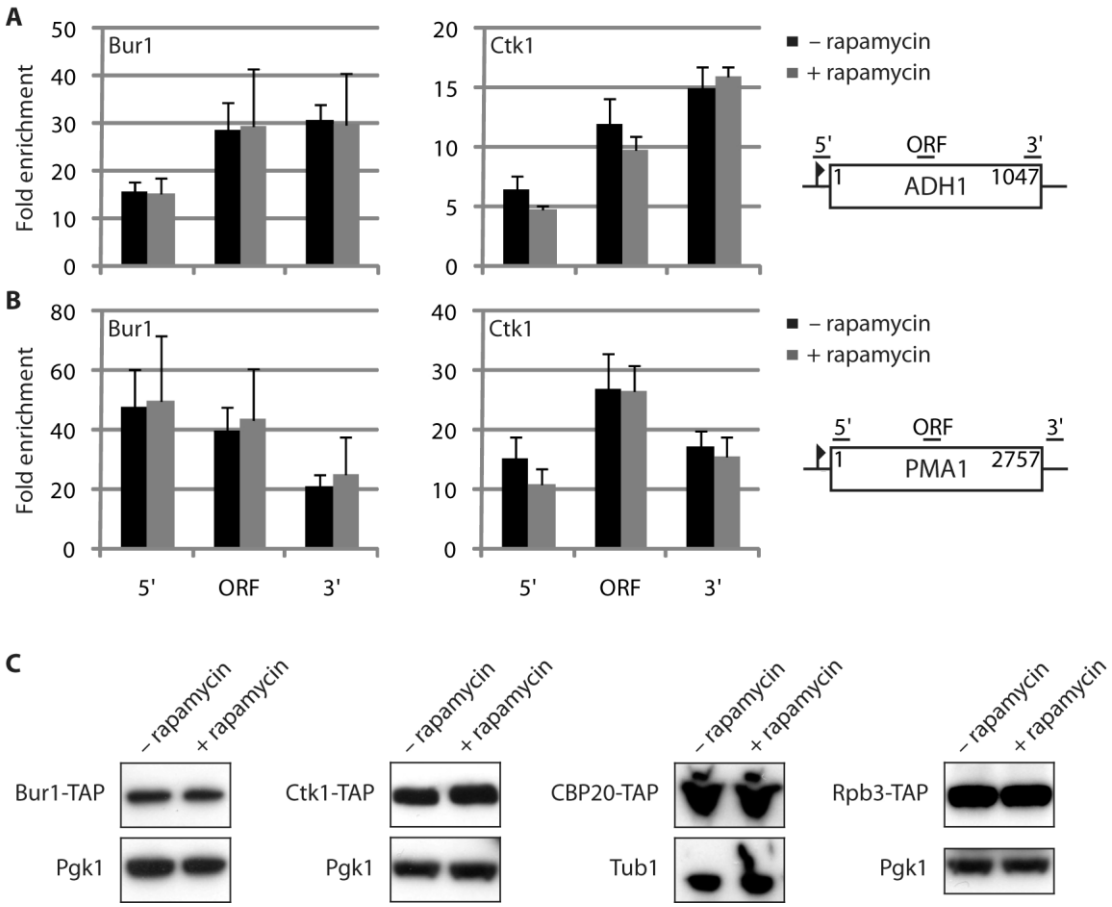

Figure S6 Rapamycin treatment does not affect Bur1 or Ctk1 occupancy at (**A**) *ADH1* and (**B**) *PMA1* using a control strain. ChIP-qPCR analysis was performed to monitor Bur1 and Ctk1 recruitment at the indicated gene regions. Occupancies in the anchor-away parental strain that was not (black bars) or was (gray bars) treated with rapamycin for 60 min are shown. Fold enrichments over an ORF-free untranscribed region on chromosome V are indicated on the y-axes (see Methods). Error bars show SD from three independent experiments of biological replicates. (**C**) Western blot analyses showing equal levels of Bur1-TAP, Ctk1-TAP, CBP20-TAP and Rpb3-TAP before and after depletion of Abd1 from the nucleus upon rapamycin treatment for 60 min. 40 µg of total protein were loaded from each strain. Pgk1 and Tub1 are included as an internal loading control.